

# On the effects of a negative step in pressure fluctuations at the bottom of a hydraulic jump

## Sur les effets d'une marche négative du fond sur les fluctuations de pressions près du fond dans des ressauts hydrauliques

V. ARMENIO, P. TOSCANO, and V. FIOROTTO, *Dipartimento di Ingegneria Civile, Sezione Idraulica e Geotecnica, Piazzale Europa 1, 34127 Trieste, Italy*

### SUMMARY

Experimental evidence of the statistical structures of turbulence pressure fluctuations at the bottom of hydraulic jumps over a negative step is brought out in this paper.

Special attention is paid to the definition of the extreme values and of the spatial correlation structures of the anisotropic field of fluctuating pressures in view of their relevance in the structural design of the lining in spillway stilling basins.

The analysis is performed in the case of *B*-jump and *Wave*-jump considering two different heights of the drop for Froude numbers ranging between 6 and 9.5. Moreover, the effect of the shape of the drop on the hydraulic jump has been investigated using the abrupt step as well as the rounded one. The experimental results herein reported may be helpful in the design of a stilling basin with a negative step, with particular reference to the thickness of the concrete slabs required to ensure the stability of the linings.

### SOMMAIRE

L'analyse expérimentale des structures statistiques de fluctuation turbulente au fond des ressauts hydrauliques par-dessus des marches négatives, est exposée.

L'attention est portée sur les positions extrêmes des phénomènes ainsi que sur les structures de corrélation spatiale du champ anisotropique de fluctuation de pression, pour permettre la réalisation d'un projet de revêtement d'un bassin amortisseur.

L'analyse a été réalisée dans le cas d'un ressaut de type "*B*" et de type "*Wave*", considérant deux différentes hauteurs de marche négative, pour nombres de Froude compris entre 6 et 9.5.

En particulier, l'effet des différentes formes de marches négatives a été analysé, en utilisant soit un abaissement brusque, soit une forme plus arrondie. Les résultats exposés peuvent être très utiles pour un projet de bassin amortisseur par-dessus une marche négative, surtout pour ce qui concerne l'épaisseur des dalles en béton nécessaires à la stabilité du revêtement.

## 1 Introduction

A drop in stilling basins is used when the downstream depth is larger than the sequent depth for a classic jump in order to ensure the jump occurrence. Furthermore, the effectiveness of a drop in the stabilization of the hydraulic jump for a wide range of the downstream depth values has been widely established (Moore and Morgan, 1959).

Figure 1 shows several types of jump at an abrupt drop in a stilling basin for a given supercritical upstream flow with mean velocity  $v_1$  and depth  $y_1$ . If the tailwater depth ( $y_2$ ) is relatively large, the hydraulic jump is located in the upstream channel; this type of jump is called *A*-Jump (*A<sub>j</sub>*). If the depth  $y_2$  is reduced, the *A<sub>j</sub>* is replaced by a wave that occurs at the drop. The supercritical stream is lifted up as a wave getting higher than the tailwater depth  $y_2$ ; due to its own shape, this jump is called *Wave*-Jump (*W<sub>j</sub>*). A further reduction of  $y_2$  makes the *W<sub>j</sub>* to turn into a *B*-Jump (*B<sub>j</sub>*) with the toe located near the drop.

The use of a jump for the dissipation of energy in a spillway basin may produce some undesired effects (Di Santo et al., 1995). In fact, accidents occurred at spillway chutes and basins while operating under flood conditions, have shown that turbulent pressure fluctuations beneath hydraulic jumps may be responsible for the loss of stability of the slabs.

Typical examples are the damages occurred at the spillway stilling basins of Malpaso and Karnafuli dam (Sanchez and Viscaïno, 1973; Bowers and Tsai, 1969).

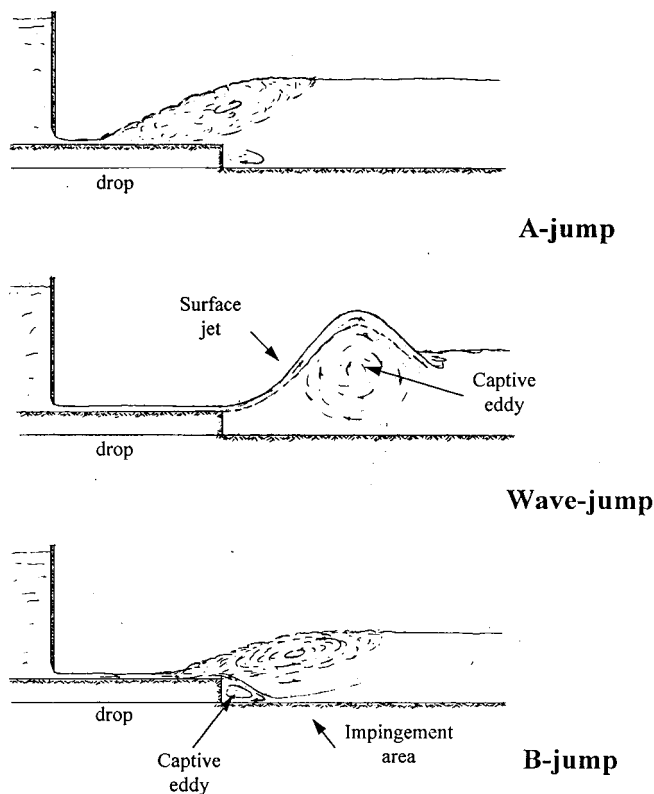


Fig. 1. Hydraulic jumps over a negative step.

Revision received July, 1999. Open for discussion till April 30, 2001.

It is well established that the failure process is due to the severe pulsating pressures in the hydraulic jump region, in particular it has been detected that:

- the pulsating pressures may damage the joint seal of the slabs and, through the unsealed joints, extreme pressure values may propagate from the upper to the lower surface of the slabs;
- the instantaneous difference between the total pressure acting on the upper and lower surfaces of the slab can reach high values, occasionally causing the total uplift force to exceed the weight of the slab.
- the instantaneous spatial structure of pressure fluctuations may play a relevant role in the magnitude of the overall lifting force.

Recently, Fiorotto and Rinaldo (1992a) proposed a design criterion for the maximum thickness of the slabs based on the magnitude of the uplift force induced by severe fluctuations associated with energy dissipation in the hydraulic jump region:

$$s > \Omega \left( \frac{l_x}{y_1}, \frac{l_x}{l_x}, \frac{l_y}{l_y} \right) (c_p^+ + c_p^-) \frac{v_1^2}{2g} \frac{\gamma}{\gamma_c - \gamma} \quad (1)$$

In Eq. 1  $s$  is the thickness of the slab,  $\Omega$  is the dimensionless reduction factor;  $l_x, l_y$  are the longitudinal and transversal length of a single slab, or the span between the joints;  $l_x, l_y$  represent the longitudinal and transversal integral scale of pressure fluctuations whereas  $\gamma$  and  $\gamma_c$  are the specific weight of water and concrete, respectively. The coefficients  $c_p$  are derived from the following relations:

$$\frac{\Delta p_{max}^+}{\gamma} = c_p^+ \frac{v_1^2}{2g} \quad \frac{\Delta p_{max}^-}{\gamma} = c_p^- \frac{v_1^2}{2g} \quad (2)$$

where  $\Delta p_{max}^+$  and  $\Delta p_{max}^-$  are respectively the maxima of the positive and negative pressure fluctuations, measured with reference to the mean value.

The use of Eq. 1 as an engineering tool requires the evaluation of the maximum negative and positive fluctuating pressures as well as of the reduction factor  $\Omega$ .

It plays a relevant role in the definition of the maximum uplift force as a function of  $l/l$ . As previously pointed out, the uplift force is due to the instantaneous pressure differentials that occur between the upper and the under surface of the slab. The pressure field beneath the slab depends on the fluctuating pressures forced through the joints at the tips of slab. If  $l/l$  vanishes the pressure field over and under the slab is fully correlated, hence the uplift force as well as  $\Omega$  tend to zero.

The increase of  $l/l$  reduces the correlation of pressure field over the slab with that along the joints, thus instantaneous maximum pressures can occur along the joints while the upper part of the slab is experiencing an instantaneous minimum of the pressure fluctuation: this circumstance makes the  $\Omega$  coefficient, and consequently the uplift force, to reach a maximum value. In a recent experimental investigation, Bellin and Fiorotto (1995) have found out  $\Omega$  to range between 0.05 and 0.25 for  $0.5 \leq l_x/l_y, l_y/l_y \leq 2.0$  depending on the slab's shape, though it has been also showed that  $\Omega$  can reach even larger values. Indeed, Fiorotto and Rinaldo (1992a) theoretically found out an estimated upper

bound of  $\Omega$  as large as 0.75, pointing out the importance of the experimental evaluation of the correlation function of the pressure fluctuations in the design of the lining slabs in stilling basins via Eq. 1.

In the past, several authors have experimentally analyzed the statistical characteristics of the fluctuating pressures beneath a classic hydraulic jump: among them, Abdul and Elango (1974), Toso and Bowers (1988), Lopardo and Henning (1985), Vasiliev and Bukreyev (1967), Fiorotto and Rinaldo (1992b). These works have dealt with the evaluation of the statistics needed for the estimation of the slab thickness *via* Eq. 1, namely standard deviation, skewness and kurtosis, maximum and minimum value, and temporal and spatial correlation of the pulsating pressures.

The transition from supercritical to subcritical flow at a drop has been extensively investigated with reference to the mean hydraulic quantities, though the evaluation of high order statistics has not extensively carried out. In particular, Moore and Morgan (1959) studied the occurrence of different shapes of hydraulic jump at an abrupt drop in a rectangular channel. They highlighted the role of the drop in the determination of the type of jump and in the stabilization of its position along the channel. They also found out that the jump configuration is strictly dependent on three dimensionless parameters, respectively the Froude number (hereafter also referred to as  $Fr$ ) of the incident flow, the relative height of the drop  $d/y_1$  and the downstream head  $y_2/y_1$ . The threshold value of the downstream head at which  $A_j, B_j$  and  $W_j$  were observed, for several heights of the drop and Froude numbers of the incident flow was also reported. Finally, measurements of the mean velocity near the bottom of the channel were performed by means of a pitot tube and reported in the paper.

The effect of a rounded edge has been investigated by Sharp (1974). The author observed that, by rounding the edge of an abrupt step, the formation of  $W_j$  can be greatly inhibited, and definitively eliminated at Froude numbers of the incident flow larger than 3.5.

Rajaratnam and Ortiz (1977) investigated the hydraulic characteristics of either  $B_j$  and  $W_j$ . The analysis of the mean velocity and pressure field, water level and shear stresses at the bottom supplied a comprehensive description of the phenomenon.

$B_j$  in prismatic stilling basins was investigated by Hager (1985) who considered the effective pressure distribution and the internal flow process. The analysis allowed a deeper understanding of the relation for the conjugate flow depths, as compared to the traditional approach.

Hager and Bretz (1986) carried out experimental investigations of the hydraulic flow features associated with hydraulic jumps either for upstream negative steps and for the downstream positive steps. The range of depth-ratios and relative-lengths representative of these types of jump were analyzed with particular attention to the design of stilling basins.

Quraishi and Al-Brahim (1992) analyzed the same flows as those studied by Hager and Bretz (1986) but in the case of sloping channels.

Ohtsu and Yasuda (1991) presented a systematic investigation on the characteristics of a hydraulic jump over a wide range of negative steps ( $0.45 \leq d/y_1 \leq 20$ ) for Froude numbers of the inci-

dent flow smaller than 5. All cases were studied theoretically by the use of the momentum equation in conjunction with measurements of the pressure distribution over the face of the drop. The analysis of the experimental results allowed to understand how the geometric characteristics of the jump affect the relevant hydraulic parameters; these findings may be useful in the hydraulic design of the stilling basins.

The previously mentioned works greatly contributed to improve the hydraulic design of the stilling basin, nevertheless they are of minor help in the structural design of the linings. For this purpose the definition of the statistical characteristics of the pulsating pressures beneath a hydraulic jump is required, and, to our knowledge, no work can be found in literature toward this direction.

This paper presents the results of an experimental investigation undertaken to evaluate the statistical parameters of the pressure fluctuations beneath a  $Bj$  as well as a  $Wj$  in order to evaluate the thickness  $s$  of the slabs by means of Eq. 1.

The paper is organized as follows: In the next section the experimental setup is described together with the flow conditions investigated. Section 3 reports the results of the experimental analysis. Finally, in section 4 some conclusions are outlined.

## 2 Experimental setup

The experiments were carried out at the Hydraulic Laboratory of the University of Trieste. A rectangular 0.96 m wide, 1 m deep and 6 m long flume was used (Fig. 2). At the upstream section a sliding gate was used to control the hydrodynamic characteristics of the incoming flow, whereas the position of the jump along the test area was controlled by a gate at the downstream end of the flume. At the bottom series of pressure taps with diameter 0.002 m were made along the center of the flume in the streamwise direction as well as at 4 different cross-stream sections (Fig.2). In order to get accurate evaluations of the spatial correlation functions the distance between two successive taps was chosen equal to 0.04 m.

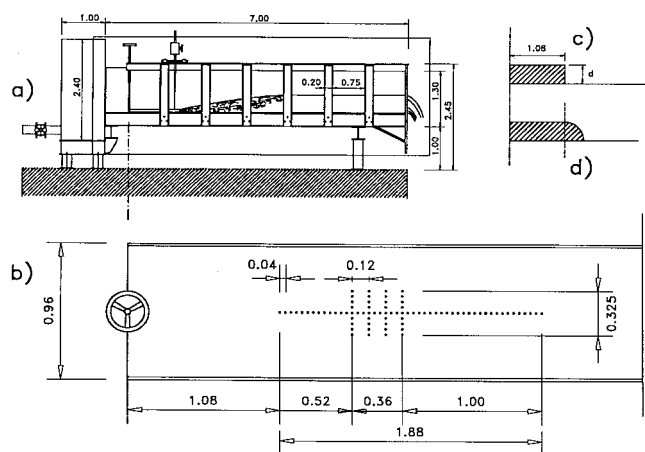


Fig. 2. Schematic of the experimental setup a) side view of the flume; b) plane view of the test area with indication of the tap positioning; c) abrupt drop and d) rounded step profile.

The fluctuating pressure at the bottom was measured by means of Transamerica Instruments BHL 4600B pressure transducers, calibrated in the range 0–250 mbar. In the linear working-range

(25–225 mbar) the transient time to the Heaviside function with amplitude of 50 mbar was smaller than the microscale time of the fluctuating pressures as measured in previous experimental works (Fiorotto and Rinaldo, 1992b). The pressure transducers were connected to the taps by 0.5 m long rigid tubes with internal diameter equal to 0.004 m.

A computer was linked to the transducer via a 16-channel A-D board Data Translation 2801A. Sampling was accomplished by Global Lab software licensed by Data Translation. Since previous spectra analyses of comparable signals had shown that the dominant frequencies of pressure fluctuations were within 30 Hz (Bendat and Piersol, 1971), a sampling rate of 100 Hz was chosen. The data were then stored on a permanent magnetic support, and processed to compute the statistics. The discharge was evaluated in the inflow pipe with a magnetic flow-meter MUT 2200 316L Automazioni Industriali.

Due to the fluctuation of the jump toe and the presence of cross waves downstream the gate, particular attention was devoted to the measure of the upstream mean depth of the water, this one needed to compute the parameters of the bulk flow.

The estimated error in the Froude number of the incident flow including the effects of discharge, depth and channel geometry amounts to a maximum of 4%, whereas the error in the kinetic head was estimated smaller than 7%.

The experiments were carried out using two different shapes of drop and two different heights of the step. First, the classic hydraulic jump was investigated with the aim to check the experimental setup by comparing the results with data available in literature. Then, the influence of the drop on the pulsating pressures at the bottom of stilling basins was analyzed.

The heights of the steps were chosen equal to 0.035 m and 0.135 m that roughly correspond to  $d/y_1 \approx 1$  and 4 respectively. Two shapes of the drop were tested, respectively an abrupt drop and a rounded step (Fig. 2).

Care was taken to eliminate possible sources of distortion in the transducer output, in particular the effect of entrapped air inside the tube and pressure cells, vibration of the bottom of the flume and the non uniform distribution of the flow across the flume.

## 3 Experimental analysis and discussions

With the assumption that the process we are going to study is stationary in time and ergodic, the following statistical properties can be evaluated:

The mean value of the pressure

$$\bar{p}(x, y) = \lim_{T \rightarrow \infty} \frac{1}{T} \int_0^T p(x, y, t) dt \quad (3)$$

and the space-time covariance function

$$R(x, \xi, y, \eta, \tau) = \lim_{T \rightarrow \infty} \frac{1}{T} \int_0^T p'(x, y, t) p'(x + \xi, y + \eta, t + \tau) dt \quad (4)$$

where  $p'(x, y, t) = p(x, y, t) - \bar{p}(x, y)$ .

The variance is defined as  $\sigma_p^2(x, y) = R(x, 0, y, 0, 0)$ , whereas the auto-covariance function is  $R(x, 0, y, 0, \tau)$  and the space instantaneous covariance is  $R(x, \xi, y, \eta, 0)$ ; the latter defines the instantaneous spatial persistence of the fluctuating pressures between any two points. Relatively to the central axis ( $y = 0$ ), the correlation surface is then defined by

$$\rho(x, \xi, 0, \eta, 0) = \frac{R(x, \xi, 0, \eta, 0)}{\sigma_p(x, 0)\sigma_p(x + \xi, \eta)} \quad (5)$$

The space macroscale in a direction (say  $x$ ) physically supplies a rough estimation of the averaged distance at which two instantaneous values of the fluctuating pressures are considered to be correlated. It reads

$$I_x = \int_0^{\infty} \rho(x_0, \xi, 0, 0, 0) d\xi \quad (6)$$

The above mentioned functions are needed to quantify the turbulent characteristics of the flow together with the frequency distribution and the maxima of the positive and negative pressure pulses  $\Delta p_{\max}^+$  and  $\Delta p_{\max}^-$ .

In Table 1 the characteristics of the bulk flow are reported. These parameters were kept constant for each experiment whereas the height and shape of the drop were changed.

The distance of the toe of the jump from the upstream gate ranged between 28 and 31 times the gate opening, hence a condition of a fully developed boundary layer could not be reached (Wilson and Turner, 1972). For classic hydraulic jump, it is established that this flow condition tends to increase the value of the standard deviation and slightly to decrease  $c_p^+$  and  $c_p^-$  (Toso and Bowers, 1988).

Table 1. Experimental parameters of the bulk flow.

Froude number	$v(m/s)$	$y_1(m)$	Reynolds number
9.5	5.31	0.032	170 000
8.0	4.65	0.0344	160 000
6.0	3.42	0.0327	112 000

Figures 3–5 show the standard deviation  $\sigma_p$  of the pulsating pressures, made dimensionless with the kinetic head

$$c_p' = \frac{\sigma_p/\gamma}{v_1^2/(2g)}$$

for three different Froude numbers. The following cases are reported: 1) classic hydraulic jump ( $Cj$ ); 2)  $B$ -jump for  $d/y_1 \approx 1$ , abrupt drop ( $ad-1 Bj$ ), 3)  $B$ -jump for  $d/y_1 \approx 1$ , rounded-step drop ( $rs-1 Bj$ ), 4)  $B$ -jump for  $d/y_1 \approx 4$ , abrupt drop ( $ad-4 Bj$ ), 5)  $B$ -jump for  $d/y_1 \approx 4$ , rounded-step drop ( $rs-4 Bj$ ) and 6) Wave-jump for  $d/y_1 \approx 4$ , abrupt drop ( $ad-4 Wj$ ).

When the characteristics of the incoming flow are kept unchanged, the range of  $y_2/y_1$  for the occurrence of  $Wj$  increases with the value of  $d/y_1$  (Moore and Morgan, 1959) and it depends on the shape of the drop (Sharp, 1974). In particular, an abrupt drop with  $d/y_1 \geq 4$  allows to get stable  $Wj$  configurations within

a wide range of  $y_2/y_1$  of practical interest (see also Moore and Morgan, 1959, pp.512, Fig.3).

A sampling time of 328s ( $2^{15}$  points according to the use of FFT) was adopted to obtain the results above reported; the maximum error in the standard deviation of the fluctuating pressure was experienced to be smaller than 4%. In order to control the quality of the measurements and to reject those affected by experimental errors, at each location at least three different pressure measurements were carried out. Figures 3–5 also report the position of abrupt drop as well as of the tip of the rounded step referred to the location of the toe of the jump. The knowledge of such locations may be useful as a reference for further experimental investigations by other authors.

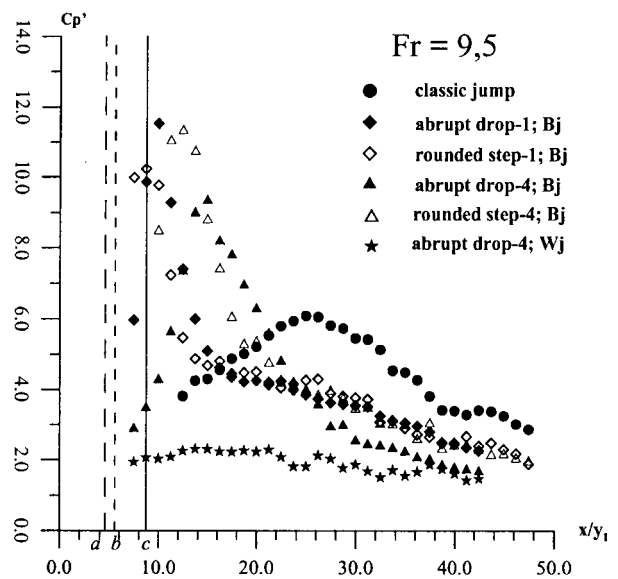


Fig. 3.  $c_p'$  coefficient along the jumps for  $Fr = 9.5$ . Locations of the steps: a, abrupt drop; b, toe of the rounded step for  $d/y_1 = 1$ ; c, toe of the rounded step for  $d/y_1 = 4$ .

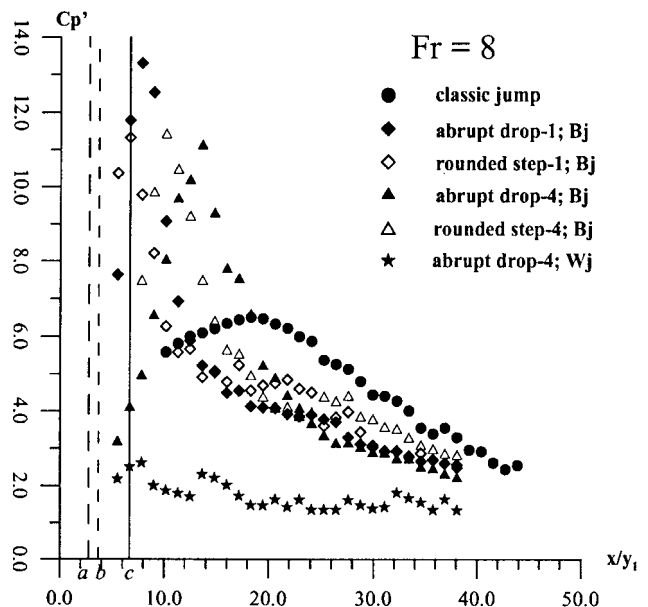


Fig. 4.  $c_p'$  coefficient along the jumps for  $Fr = 8.0$ . Locations of the steps: a, abrupt drop; b, toe of the rounded step for  $d/y_1 = 1$ ; c, toe of the rounded step for  $d/y_1 = 4$ .

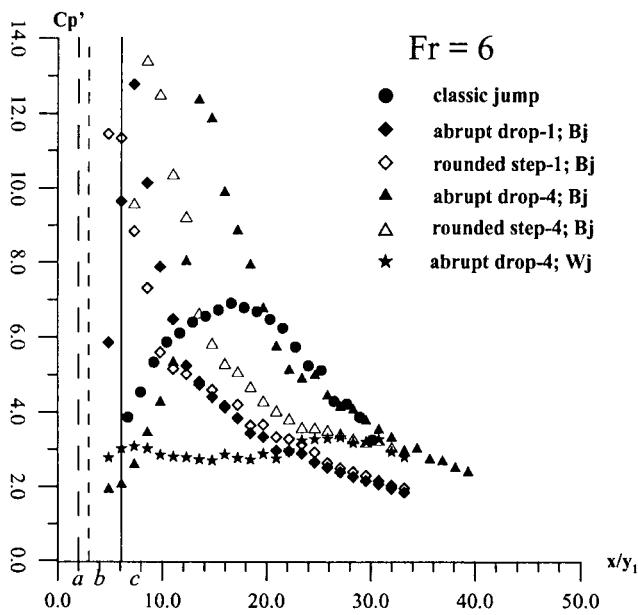


Fig. 5.  $c_p'$  coefficient along the jumps for  $Fr = 6.0$ . Locations of the steps: a, abrupt drop; b, toe of the rounded step for  $d/y_1 = 1$ ; c, toe of the rounded step for  $d/y_1 = 4$ .

For  $C_j$ , the  $c_p'$  coefficients are in good agreement with the data of Fiorotto and Rinaldo (1992 b) and Toso and Bowers (1988) for not fully developed flow. Some discrepancies in the results among different investigations may be due to experimental uncertainties, e.g. the difficulty to evaluate the distance of the pressure taps from the jump toe and in the measure of the water depth at the inflow. As regards  $B_j$  it was observed that :

- i in the upward part of the  $B_j$  the pressure coefficient is higher if compared to  $C_j$ ;
- ii the pressure coefficient gets maximum in the impingement region, then it decreases reaching smaller values than in  $C_j$ ;
- iii in the case of a rounded step, the increase of the height of the step produces larger values of  $c_p'$  and, moreover, the zone where these coefficients are larger than in  $C_j$  widens.
- iv in the case of an abrupt step, the increase of the height of the step produces smaller values of  $c_p'$ ; similarly to iii) the zone where these coefficients are larger than in  $C_j$  widens;
- v the distance from the toe of the jump at which the stream impacts the channel bottom, the height of the step being kept constant, is larger in the abrupt drop case as compared to the rounded step where the supercritical stream is driven by the step shape; this is more evident if the height of the step increases;
- vi downstream the impingement zone, the pressure coefficients are to a large extent independent on the step height and their values are smaller than in  $C_j$ ;
- vii The above mentioned effects are nearly independent on the Froude number of the incident flow.

These issues can be explained as follows: the presence of the negative step forms a captive eddy which dissipates a significant part of the energy of the incoming flow. The supercritical stream behaves like a plane turbulent jet, soon it turns into a curved jet sandwiched between the surface roller on the top and the captive

eddy on the bottom, and eventually it impinges on the bed of the downstream channel. From the impingement area, where the maximum fluctuating pressure occurs, the flow grows as a turbulent wall jet up to the end of the surface roller and then gradually degenerates into a fully developed subcritical flow.

In the case of an abrupt drop the increase of the step height causes the captive eddy to get larger and more intense than in the rounded step case (Fig. 3-5); the rate of energy dissipated upstream the impingement zone becomes larger than the rate of energy gained when the step height is increased, thus an overall reduction of the maximum pressure fluctuations is observed.

On the other hand, a rounded step causes the maximum pressure fluctuations to increase with the step height. This occurs because the upstream flow is driven by the step shape and the energy dissipated before the impact over the bottom of the channel gets smaller than the rate of energy gained with the increase of the step height.

Finally it is noteworthy observing that, when a  $W_j$  develops the  $c_p'$  coefficients are smaller and smoother if compared with both  $C_j$  and  $B_j$ .

The experiments indeed show that the supercritical stream is lifted up as a surface jet at the top of a large captive eddy, thus resulting into a wave. This eddy is generated by the pressure field close to the drop. Then, the surface jet plunges into the tailwater and impinges upon the bed downstream the eddy. This large recirculation behaves like a "water-cushion" which prevents from the generation of large pressure fluctuations at the bottom of the channel. For  $W_j$  only the abrupt drop is studied, because a rounded edge inhibits the formation of the jump (Sharp, 1974).

In order to evaluate the magnitude of the extreme values of the pressure fluctuations, long-duration experiments were performed. These were accomplished with the aim to define an upper bound to the pulsating pressure based on the assumption that the energy content in the jump is limited and therefore a practical limit to the magnitude of pressure pulses must be obtained. In practical applications for high velocities of the incoming flow the lower pressure limit could be bounded by cavitation phenomena. In Fig. 6-8 the time history of  $c_p^+$  and  $c_p^-$ , measured in the zone where the maximum value of the  $c_p'$  occurs, are shown.

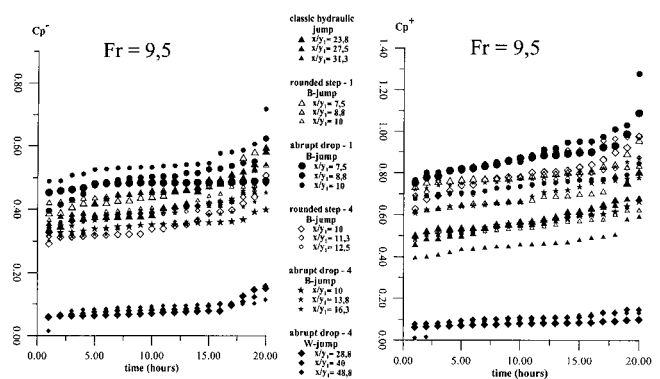


Fig. 6. Effect of run-time on negative and positive pressure peak deviation from mean value for  $Fr = 9.5$

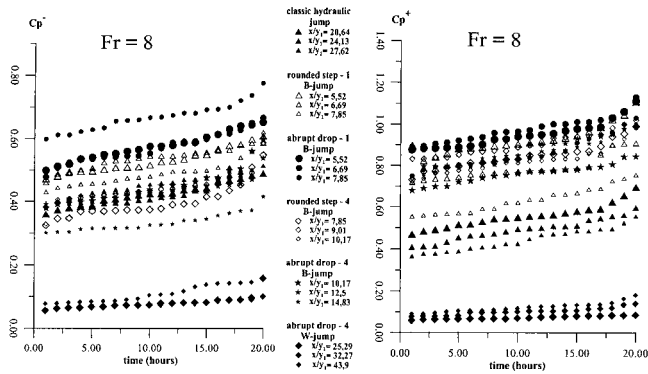


Fig. 7. Effect of run-time on negative and positive pressure peak deviation from mean value for  $Fr = 8.0$

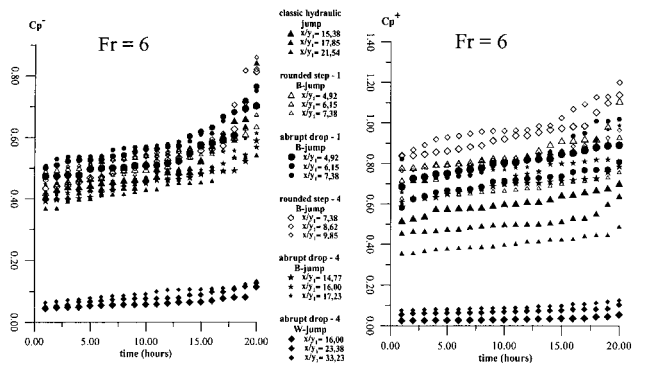


Fig. 8. Effect of run-time on negative and positive pressure peak deviation from mean value for  $Fr = 6.0$

The analysis of the Figures suggests that the upper and lower limits were not reached, in fact a significant increase was observed even for a total sampling time equal to 20 hours. However, the practical value of these coefficients may be evaluated as the maximum value in a sufficient long-time model-scale experiment with respect to the probable duration of the discharge event in the prototype: for instance, 20 hours in a 1:100 scale-model correspond to a 8-day event in the prototype. Table 2 reports the maximum values of  $c_p^+$  and  $c_p^-$ .

The maximum value of the compound coefficient  $c_p^+ + c_p^-$  can be derived, and it clearly appears that for Bj it is larger than  $Cj$ . With reference to Eq. 1 it can be detected that the Bj stilling basins may require slab thicknesses larger than the  $Cj$  ones.

For  $Wj$  case the pressure measurements herein reported were obtained in the zone downstream the captive eddy, namely where the surface jet impinges on the bed. It appears that  $c_p^+$  and  $c_p^-$  get the same order of magnitude and they are much smaller than that measured both in  $Cj$  and in  $Bj$ . As a consequence, the use of Eq. 1 shows that the  $Wj$  stilling basins may require smaller thickness of the protections.

With reference to  $Bj$ , the positive fluctuating pressure coefficients  $c_p^+$  can reach values larger than unity and  $c_p^+$  is always larger than  $c_p^-$  (Table 2), thus producing significant lack of symmetry in the probability density function (pdf) of the fluctuating pressure. It follows that the pdf cannot be represented with a Gaussian one, making difficult to assess a probability level associated with  $c_p^+$

and  $c_p^-$  given the  $c_p^-$  value. In Fig. 9 a comparison between experimental frequency distributions and the Gaussian distribution is shown in the zone where the maximum differences in pressure occurs for  $Fr = 8.0$ . In Fig. 9 skewness and kurtosis are also reported. It is clearly shown that in  $Bj$  the positive fluctuating pressures are relatively more frequent than the negative ones. The experimental pdf for  $Wj$  better fits the Gaussian pdf, indeed the skewness is vanishingly small whereas the kurtosis is close to 3.

Table 2. Maximum value of  $c_p$  coefficients measured in long test runs (20 hours).

Fr	$x/y_1$	jump	$Cp^-$	$Cp^+$
9.5	23.8	classic jump	0.583	0.807
	27.5	classic jump	0.597	0.846
	31.3	classic jump	0.544	0.593
	7.5	rounded step-1 B jump	0.595	0.958
	8.8	rounded step-1 B jump	0.541	0.838
	10	rounded step-1 B jump	0.488	0.624
	7.5	abrupt drop-1 B jump	0.489	1.09
	8.8	abrupt drop-1 B jump	0.623	1.28
	10	abrupt drop-1 B jump	0.717	0.847
	10	rounded step-4 B jump	0.506	0.976
	11.3	rounded step-4 B jump	0.482	0.981
	12.5	rounded step-4 B jump	0.488	0.875
8	10	abrupt drop-4 B jump	0.398	0.664
	13.8	abrupt drop-4 B jump	0.484	0.778
	16.3	abrupt drop-4 B jump	0.453	0.870
	28.8	abrupt drop-4 W jump	0.15	0.099
	40	abrupt drop-4 W jump	0.157	0.147
	48.8	abrupt drop-4 W jump	0.114	0.132
	20.64	classic jump	0.489	0.697
	24.13	classic jump	0.666	0.596
	27.62	classic jump	0.514	0.556
	5.52	rounded step-1 B jump	0.608	1.107
	6.69	rounded step-1 B jump	0.586	0.909
	6	7.85	rounded step-1 B jump	0.621
5.52		abrupt drop-1 B jump	0.652	1.11
6.69		abrupt drop-1 B jump	0.666	1.13
7.85		abrupt drop-1 B jump	0.775	1.03
7.85		rounded step-4 B jump	0.548	0.990
9.01		rounded step-4 B jump	0.587	1.02
10.17		rounded step-4 B jump	0.604	0.995
10.17		abrupt drop-4 B jump	0.597	0.845
12.5		abrupt drop-4 B jump	0.538	0.986
14.83		abrupt drop-4 B jump	0.415	1.0
25.29		abrupt drop-4 W jump	0.158	0.085
32.27		abrupt drop-4 W jump	0.101	0.139
43.9	abrupt drop-4 W jump	0.163	0.179	
6	15.38	classic jump	0.706	0.702
	17.85	classic jump	0.843	0.639
	21.54	classic jump	0.543	0.489
	4.92	rounded step-1 B jump	0.706	1.11
	6.15	rounded step-1 B jump	0.636	0.931
	7.38	rounded step-1 B jump	0.675	0.759
	4.92	abrupt drop-1 B jump	0.702	0.891
	6.15	abrupt drop-1 B jump	0.765	0.808
	7.38	abrupt drop-1 B jump	0.751	1.02
	7.38	rounded step-4 B jump	0.814	1.14
	8.62	rounded step-4 B jump	0.822	1.202
	9.85	rounded step-4 B jump	0.861	0.966
14.77	abrupt drop-4 B jump	0.590	0.785	
16.0	abrupt drop-4 B jump	0.569	0.891	
17.23	abrupt drop-4 B jump	0.614	0.989	
16.00	abrupt drop-4 W jump	0.115	0.0533	
23.38	abrupt drop-4 W jump	0.127	0.0806	
33.23	abrupt drop-4 W jump	0.132	0.112	

For practical purposes, in  $Wj$ , the reduction coefficient  $\Omega$  can be computed via standard deviation of the force acting on the slab assuming the frequency distribution of the pulsating pressure to be Gaussian (Bellin and Fiorotto, 1995). For  $Bj$  this procedure could lead to relevant errors; however  $\Omega$  can be directly evaluated by the use of the ratio between the slab dimensions  $l_x, l_y$  and the spatial integral scale  $l_x, l_y$  of the pulsating pressure field (Fiorotto and Rinaldo, 1992b).

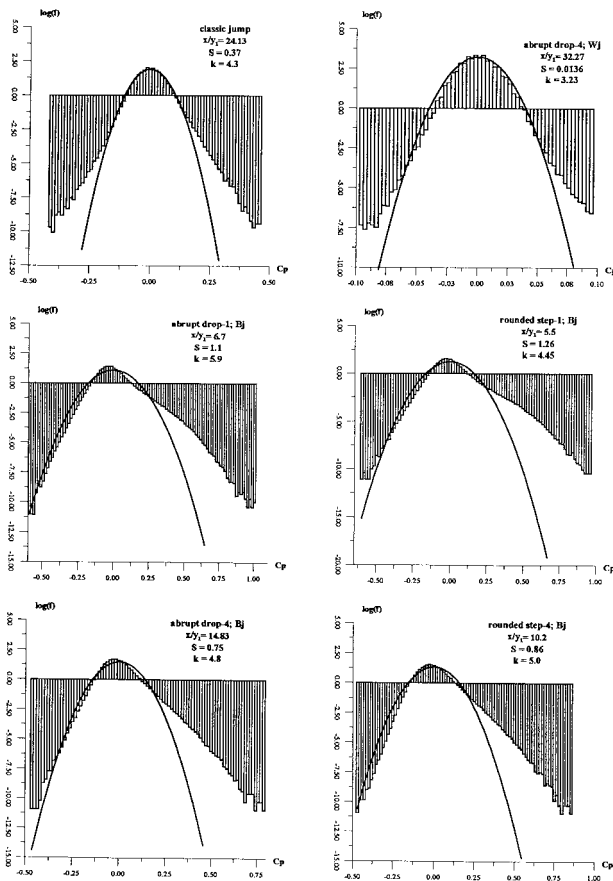


Fig. 9. Probability density function  $f$  of pressure fluctuations compared to the normal distribution in the location where the maxidevelopsmum pressure fluctuations occur.

The evaluation of  $\Omega$  requires the calculation of the correlation functions along the flow direction and in the transversal direction. A sampling time of 328 s was used to compute the correlation functions and always at least three different runs were performed. The maximum error in the correlation functions resulted smaller than 3%.

It is remarkable that, since the pressure field is not statistically homogeneous along the streamwise direction, the  $c_p$ ' coefficients (Fig. 3–5) depend on the distance from the jump toe.

Figure 10 shows the longitudinal correlation at  $Fr = 9.5$ , for  $Wj$  as well as  $Bj$  with an abrupt drop ( $d \approx 4y_1$ ), and comparisons with  $Cj$ . As previously remarked, the correlation function depends on the pivot location. It appears that for  $Wj$  the correlation function has a different shape as compared to  $Bj$  and  $Cj$ , it gets only positive values and it could be fitted with an exponential function. This behavior is due to the presence of a large captive eddy characterized by a correlation length (integral scale  $I_x$ ) larger than in  $Cj$  and  $Bj$ .

The experimental results for  $Cj$  and  $Bj$  are summarized in Fig. 11. The values of the first zero-crossing distance  $\xi_0$  are reported as a function of the pivot point. As shown by Fiorotto and Rinaldo (1992b), this distance can be reasonably assumed proportional to the streamwise correlation length ( $I_x \approx 0.2\xi_0$ ). The analysis of the Figure shows that:

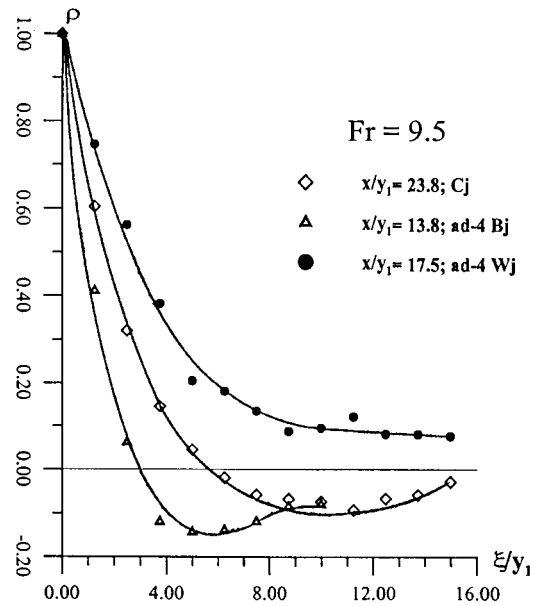


Fig. 10. Longitudinal correlation function for  $Fr = 9.5$ .

a) in  $Cj$ :

- i) as long as the Froude number is kept constant, the distance of the zero crossing-point does increase when the distance of the pivot point from the toe of the jump increases;
- ii) the distance of the zero crossing-point does increase when the Froude number increases. The experimental results here reported are in good agreement with the data of Lopardo and Henning (1985), Vasiliev and Bukreyev (1967) and Fiorotto and Rinaldo (1992 b).

b) in  $Bj$ :

- i) the distance of the zero crossing-point has a minimum in the impingement zone where the maximum pressure fluctuations occur; (the locations where the maximum value of  $c_p$ ' occurs are also indicated in the Figures)
- ii) the integral scale of the fluctuating pressure increases going upstream, because of the presence of the captive eddy. This fact is particularly clear for the case  $d \approx 4y_1$ , characterized by a very large extension of the recirculation zone;
- iii) the same phenomenon is observed downstream; the zero crossing point distance does increase with the distance of the pivot point. The experimental points tend to collapse over a line parallel to that of  $Cj$ , hence behaving like a  $Cj$  but with a different Froude number.

The analysis of Fig. 11 also shows that for  $Fr = 8$  and  $Fr = 9.5$  the correlation length is reduced if compared to the  $Cj$ : this means that the energy dissipation upstream the impingement area is larger than the potential energy gained with the drop. This fact is particularly evident for  $d \approx 4y_1$ . Finally, it appears that in the abrupt drop the captive eddy is more intense and it dissipates more energy than for the rounded step case thus resulting in smaller values of  $\xi_0/y_1$ .

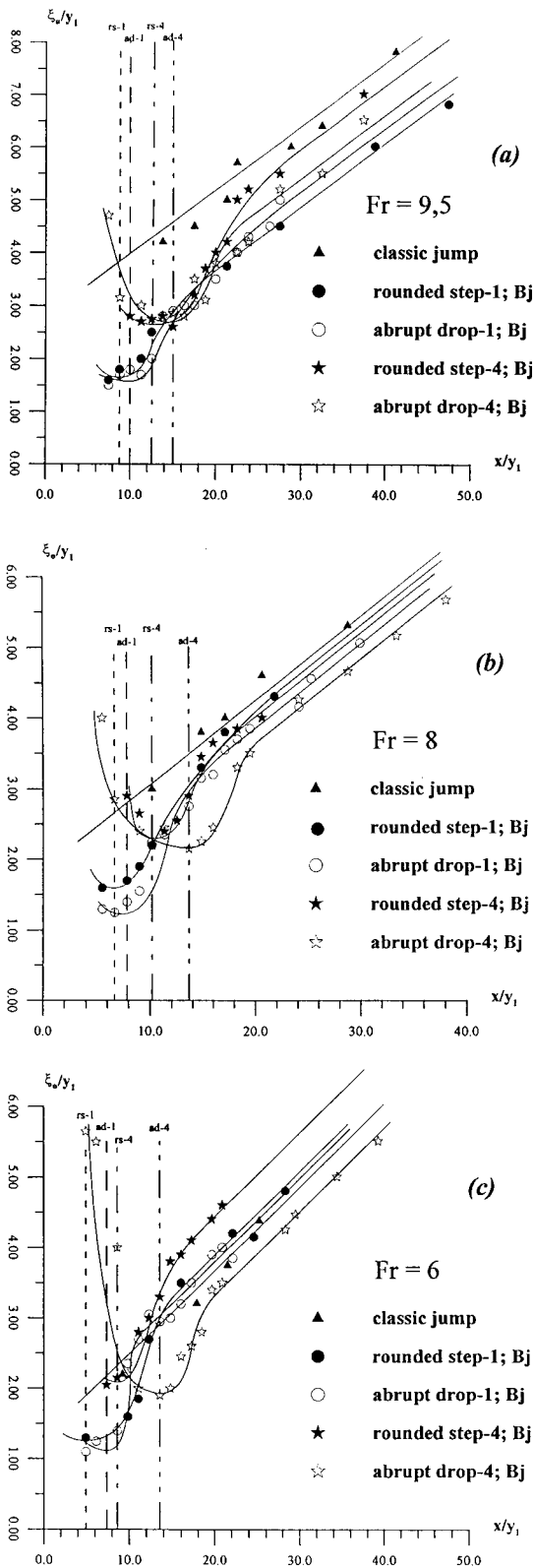


Fig. 11.  $\xi_0/y_1$  versus  $x/y_1$  for Bj and Cj. The location where the maximum occurs is also indicated : a)  $Fr = 9.5$ ; b)  $Fr = 8.0$ ; c)  $Fr = 6.0$

When  $Fr = 6$ , large differences between the abrupt drop case and rounded step case are evident for  $d \approx 4y_1$  only. The rounded step makes the recirculation zone to be very small thus energy dissipation is smaller than the potential energy gained with the drop.

In Table 3 the integral scale  $I_x$  versus the dimensionless distances  $x/y_1$  is reported for  $W_j$ . It has to be pointed out that the distance  $x$  is measured with respect to the toe of  $B_j$  and  $C_j$ : for sake of coherence the same distance is used in the case of  $W_j$ . However, the above distance can be referred to location of the abrupt drop by the use of Fig. 3–5; indeed if we indicate with  $x_d$  this distance, it is related to the distance  $x$  by:  $x_d/y_1 = x/y_1 - 4.53$  for  $Fr = 9.5$ ;  $x_d/y_1 = x/y_1 - 2.76$  for  $Fr = 8$  and  $x_d/y_1 = x/y_1 - 2.0$  for  $Fr = 6.0$ . The integral scale  $I_x$  was computed via Eq. 6 by interpolation of the experimental data with an exponential function and its behavior always shows the presence of a large captive eddy characterized by a correlation length larger than in the  $C_j$ . It can also be noticed that, for a given Froude number, the dimensionless integral scale  $I_x/y_1$  tends to decrease as long as the distance of the pivot point increases, whereas for a given value of  $x/y_1$  the dimensionless integral scale  $I_x/y_1$  increases accordingly with the Froude number.

Table 3. Longitudinal dimensionless integral scale  $I_x/y_1$  versus  $x/y_1$  in  $W_j$ .

Fr=9.5		Fr=8		Fr=6	
$x/y_1$	$I_x/y_1$	$x/y_1$	$I_x/y_1$	$x/y_1$	$I_x/y_1$
7.5	7.1	5.5	6.1	4.9	5.2
12.5	6.6	10.2	5.1	9.9	4.1
17.5	5.2	14.8	4.5	14.8	2.8
22.5	4.8	19.5	3.5	19.7	2.9
27.5	5.3	24.1	3.2	24.6	3.1

Figure 12 shows the transversal correlation  $\rho(x, 0, y, \eta, 0)$  for  $Fr = 8$  in  $C_j$ ,  $B_j$  and  $W_j$  for  $d \approx 4y_1$ . First it can be observed that the pressure field is statistically homogeneous in this direction.

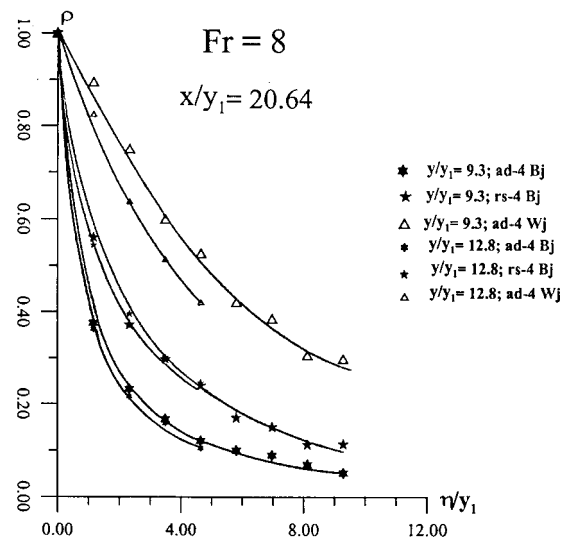


Fig. 12. Transverse correlation function for  $Fr = 8.0$  (the distance  $y/y_1$  is measured from the central line of the channel).

Then, Fig. 12 shows that the abrupt drop causes the transversal integral scale to be smaller than that obtained with the rounded step. This means (Fiorotto and Rinaldo, 1992b) that the Froude number characterizing the final part of the jump in the rounded step case is larger than in the abrupt step case, in agreement with the results reported in Fig. 11.

In this case the transversal integral scale  $I_y$  can be deduced from the longitudinal integral scale  $I_x$ ; in the present investigation the ratio  $I_y/I_x$  is experienced to lie in the range 5–6 (thus  $I_y \approx \xi_0$ ), and it appears to be practically independent on the Froude number and on the location of the pivot point along the flow direction.

In  $Wj$  the transversal integral scale  $I_y$  is larger than in  $Bj$  as well as in  $Cj$  and its value is comparable with the longitudinal integral scale  $I_x$ . The integral scale  $I_y$  (computed assuming an exponential behaviour of the transversal correlation function) lies in the range  $1.6 < I_y/I_x < 1.8$ , seemingly independent on the Froude number of the incident flow and of the distance of the pivot point  $x_d$ .

The findings of the above experimental analysis can be used in practical applications, and, for purposes of illustration the design of a stilling basin is presented in the following. The inflow depth and velocity are assumed equal to 0.75 m and 16 m/s, respectively. The resulting Froude number is 6.0. The stilling basin is built with 2.0 m width and 4.5 m long concrete slabs. Three flow configurations are herein examined, respectively  $Cj$ ,  $Bj$  in the case of rounded step with height equal to 3.0 m, and  $Wj$  with a 3.0 m height abrupt drop.

For  $Cj$  the maximum value of  $c_p^+ + c_p^-$  is equal to 1.5 at  $x/y_1 = 15.4$  (Table 2). The integral scale  $I_y$  is roughly equal to  $5I_x$  and it gets the same order of  $\xi_0$ , thus (Fig.11)  $I_y \approx 3Y_1 \approx 2.25m$  while  $I_x \approx 0.2I_y \approx 0.45m$ . It follows that  $l_y/I_y \approx 0.9$  and  $l_x/I_x \approx 10.0$ . The coefficient  $\Omega$  can be evaluated from the experimental data of Fiorotto and Bellin (1995, Fig. 5 pag. 691), thus obtaining  $\Omega \sim 0.1$ . From Eq. 1, assuming  $\gamma(\gamma_s - \gamma) = 0.66$ , we obtain  $s \approx 1.4m$ , that has to be increased to 2.0 after that an overall safety coefficient equal to 1.5 is employed.

For  $Bj$  with a rounded step with height equal to 3.0 m the maximum value of  $c_p^+ + c_p^-$  is equal to 2.02 at the location  $x/y_1 = 8.6$  (Table 2). The integral scale  $I_y \approx \xi_0 \approx 2.25y_1 = 1.7m$  (see also Fig. 11) while  $I_x \approx 0.2I_y = 0.34m$ , hence  $l_y/I_y = 1.2$  and  $l_x/I_x = 13.0$ . With these values, the coefficient  $\Omega$  is roughly equal to 0.2, and, applying the same procedure as in the previous case, we obtain the suggested design value  $s \approx 5.3m$ .

Finally, for  $Wj$ , the maximum value of  $c_p^+ + c_p^-$  is equal to 0.24 at  $x/y_1 = 33.23$  (Table 2); in this case (Table 3)  $I_x \approx 3.0y_1 = 2.25m$  while  $I_y \approx 1.6I_x = 3.5m$ , therefore we obtain  $l_y/I_y \approx 0.6$  and  $l_x/I_x \approx 2.0$ . The experimental data of Fiorotto and Bellin (1995, Fig. 5 pag. 691) provide  $\Omega$  smaller than 0.1. In this case the suggested design value is  $s \approx 0.5m$ .

This example clearly shows the role of the pressure coefficients  $c_p^+$ ,  $c_p^-$  and of the ratios  $l_y/I_y$  and  $l_x/I_x$  in the computation of the equivalent thickness of the lining, where equivalent thickness means that if the structure is anchored to underlying rock, the failure strength of the anchor must be properly transformed into equivalent weight (Fiorotto and Salandin, 1999)

#### 4 Conclusions

In this paper the pressure fluctuations beneath a hydraulic jump that develops over a negative step have been investigated. The study was carried out experimentally, using two different drops, an abrupt drop and a rounded step respectively, and varying the

inflow and outflow conditions of the flume in order to obtain a  $Bj$  and a  $Wj$ . The analysis has shown that, when a  $Bj$  develops:

- the maximum pressure fluctuations are larger than in  $Cj$ , the pressure coefficient  $c_p$  reaching values even larger than unity;
- the probability density function of the pressure fluctuations substantially differs from a Gaussian distribution, hence the use of the Gaussian hypothesis might lead to loss of accuracy in the overall estimation of the reduction factor  $\Omega$ ;
- the normalized spatial correlation is anisotropic and the length of the longitudinal correlation is smaller than that of the transversal correlation;
- the flow is not homogeneous in the streamwise direction and the longitudinal correlation experiences a minimum in the impingement location;
- the transversal correlation is homogeneous, so that the statistical characteristics of the pressure fluctuations do not depend on the  $y$  coordinate.

Conversely, when a  $Wj$  develops, it has been observed that:

- the maximum pressure fluctuations are smaller than in the case of  $Cj$ . The pressure coefficient  $c_p$  is confined within 20% the values measured in  $Cj$ ;
- the probability density function of the pressure fluctuations can be assumed reasonably Gaussian, thus this assumption can be used for the overall estimation of  $\Omega$ ;
- the extent of the longitudinal correlation is not homogeneous and it has been shown larger than in  $Cj$  according to the lacking of an actual impingement zone;
- the transverse correlation is homogeneous and it exhibits a correlation length larger than in  $Cj$ .

From Eq. 1, it results that  $Wj$  stilling basins require the slabs to be thinner than in  $Cj$ , indeed the thickness is about 25% of the thickness needed to ensure stability in the  $Cj$  stilling basins. On the contrary, the  $Bj$  stilling basins require thickness as large as three times those computed for  $Cj$ .

#### Notations

ad-1	abrupt drop with $d/y_1 \approx 1$ .
ad-4	abrupt drop with $d/y_1 \approx 4$ .
$Bj$	$B$ -jump.
$Cj$	classic jump .
$c_p$	dimensionless pressure coefficient.
$c_p'$	dimensionless standard deviation of the pulsating pressures.
$d$	height of step.
$f$ or $pdf$	probability density function.
$Fr$	Froude number.
$I_x$	longitudinal integral scale of pressure fluctuations.
$I_y$	transversal integral scale of pressure fluctuations.
$K$	kurtosis.
$l_x$	longitudinal length of the slabs.
$l_y$	transversal dimension of the slabs.
$p$	pressure field $p(x,y,t)$ .
$R$	space time double covariance function.

rs-1	rounded step with $d/y_1 \approx 1$ .	17. SHARP J.J. (1974), Observation on hydraulic jumps at rounded step, J. Hydr. Div. Vol. 100, n. HY6.
rs-4	rounded step with $d/y_1 \approx 4$ .	18. TOSO J. and BOWER E.C. (1988), Extreme pressure in hydraulic jump stilling basins, J. Hydr. Engrg. ASCE, Vol.114(8).
s	equivalent thickness of the slabs.	19. VASSILIEV O.F. and BUKREYEV V.I.(1967), Statistical characteristic of pressure fluctuations in the region of hydraulic jump, Proc. XII IAHR Congress, Fort Collins, Co.(USA), Vol.2.
S	skewness.	20. WILSON E.H. and TURNER A.A. (1972), Boundary layer effects on hydraulic jump location, J. Hydr. Div., ASCE, Vol.98, HY7.
$v_1$	average inflow velocity.	
Wj	Wave-jump.	
x	longitudinal distance from the toe of the jump.	
$x_d$	longitudinal distance from the abrupt drop.	
$y_1$	inflow depth.	
$y_2$	conjugate depth in the jump.	
y	transversal distance from the central axis.	
$\gamma$	specific weight of water.	
$\gamma_c$	specific weight of concrete.	
$\Delta p^+_{\max}$	maximum positive pressure deviation from the mean.	
$\Delta p^-_{\max}$	maximum negative pressure deviation from the mean.	
$\rho$	correlation function.	
$\sigma_p$	standard deviation of the fluctuating pressure.	
$\Omega$	dimensionless reduction factor in Eq.1.	
$\xi$	longitudinal distance from the pivot point.	
$\xi_0$	distance between the origin and the first zero crossing of the longitudinal correlation	
$\eta$	transversal distance from the pivot point	

## References

1. ABDUL KADER M.H. and ELANGO K. (1974), Turbulent pressure beneath a hydraulic jump, J. Hydr. Res., Vol.12, n. 4.
2. BELLIN A. and FIOROTTO V. (1995), Direct dynamic force measurement on slabs in spillway stilling basins, J. Hydr. Engrg., ASCE, 121, n. 10.
3. BENDAT J.S. and PERSOL, A.G.(1971), Random data: analysis and measurement procedures, J. Wiley & Sons, N.Y..
4. BOWERS C.E. and TSAI F.H. (1969), Fluctuating pressure in spillway stilling basins, J. Hydr. Div., ASCE, Vol.95, HY6.
5. DI SANTO A., PETRILLO A. F. and PICCINNI A. F. (1995), Experimental studies on the stability of lining slabs in hydraulic jumps stilling basins, EXCERPTA, Vol. 9.
6. FIOROTTO V. and RINALDO A. (1992a), Fluctuating upflit and linings design in spillway stilling basins, J. Hydr. Engrg., ASCE, Vol.118, n. 4.
7. FIOROTTO V. and RINALDO A. (1992b), Turbulent pressure fluctuations under hydraulic jumps, J. Hydr. Res., Vol.30, n. 4.
8. FIOROTTO V. and SALANDIN P. (2000), Design of anchored slabs in spillway stilling basins, submitted on J. Hydr Engrg, ASCE.
9. HAGER W. H. and BRETZ N. V. (1986), Hydraulic jump at positive and negative steps, J. Hydr. Res., Vol. 24, n. 4.
10. HAGER W. H. (1985), B-Jumps at abrupt channel drops, J. Hydr. Engrg., ASCE, vol. 111, n. 5
11. LOPARDO, R.A. and HENNING, R.E. (1985), Experimental advances on pressure fluctuation beneath hydraulic jumps, Proc., 21 st IAHR, Melbourne Australia, Vol. 3.
12. MOORE W. L. and MORGAN C. W. (1959), Hydraulic jump at an abrupt drop, Transaction ASCE, vol. 124, paper n. 2991. (with discussion by McPherson M.M. B.; Forster J. W.)
13. OHTSU, I. and YASUDA Y., (1991), Transition from supercritical to subcritical flow at an abrupt drop, J. Hydr. Res., Vol. 29, n. 3.
14. QURAIISHI A. A. and AL-BRAHIM A. M. (1992), Hydraulic jump in sloping channel with positive or negative step, J. Hydr. Res., Vol. 30, n. 6.
15. RAJARATNAM N. and ORTIZ N. V.(1977), Hydraulic jumps and waves at abrupt drops, J. Hydr. Div., ASCE, Vol. 103, HY4.
16. SANCHEZ BRIBIESCA J.S. and VISCAINO A.C.(1973), Turbulence effects on the lining of stilling basins, ICOLD 11 st Int. Congress Madrid, Q41, Vol. 2.